第27卷 第3期 半 导 体 学 报 Vol.27 No.3
2006年3月 CHINESE JOURNAL OF SEMICONDUCTORS Mar.,2006

Equivalent Circuit Analysis of an RF Integrated Inductor with Ferrite Thin-Film*

Ren Tianling[1,†], Yang Chen[1], Liu Feng[1], Liu Litian[1],
Wang A Z[2], and Zhang Xiao[3]

(1 *Institute of Microelectronics, Tsinghua University, Beijing 100084, China*)
(2 *Department of Electrical and Computer Engineering, Illinois Institute of Technology, Chicago IL 60616, USA*)
(3 *Department of Electronic Engineering, Tsinghua University, Beijing 100084, China*)

Abstract: An equivalent circuit for a novel RF integrated inductor with ferrite thin-film is derived. The enhancement of the magnetic ferrite thin-film on the inductance (L) and quality factor (Q) of the inductor is analyzed. Circuit element parameters are extracted from RF measurements. Compared with the reference air-core inductor without magnetic film, L and Q of the ferrite thin-film inductor are 17% and 40% higher at 2GHz, respectively. Both the equivalent circuit analysis and test results demonstrate significant enhancement of the performance of RF integration inductors by ferrite thin-film integration.

Key words: inductor; equivalent circuit; ferrite thin-film; RF ICs
EEACC: 2560B; 2140; 3110E
CLC number: TN409 **Document code:** A **Article ID:** 0253-4177(2006)03-0511-05

1 Introduction

Radio frequency integrated circuit (RF ICs) technology has enjoyed unprecedented advancements in recent years thanks to the rapid development of wireless communication applications. However, in the passive element area, a lack of compact, high-performance, high-frequency, on-chip RF inductors hinders the realization of RF system-on-chip (SoC) devices in commercial products. The trouble is caused by two major difficulties[1]. One is the cost of area. Typical spiral inductors usually consume large amounts of chip area compared to other on-chip components. The other is a problem of performance. Different losses due to various parasitic effects make the inductor and total circuit perform poorly. These difficulties have motivated great research efforts to develop high-performance inductors for RF IC applications. Some advances have been achieved, such as enhanced Q using special substrates[2~4] or MEMS techniques[5~6] and reduced size with stacked structures[7~8]. However, it is not easy to reduce the size and enhance the performance of the inductors simultaneously.

Integrating magnetic media as the flux-amplifying component of inductors is a new possible solution for the realization of super-compact, high-performance inductors. The greater flux linkage contained in magnetic material will increase inductance and reduce loss. As a result, inductor size can be reduced simultaneously. In Ref. [1], we used ferrite thin-film as the magnetic media and proposed a novel RF integrated inductor with ferrite thin-film. However, to date the equivalent circuit of the ferrite thin-film inductor has not yet been proposed. In this paper, the equivalent circuit analysis of the reported inductor with ferrite thin-film in Ref. [1] is performed. Circuit analysis and test results show the contribution of ferrite thin-film to the inductance (L) and the quality factor (Q) of the inductor.

* Project supported by the National Natural Science Foundation of the USA (No.0302499)

† Corresponding author. Email: RenTL@tsinghua.edu.cn

Received 7 November 2005

2 Structure

Figure 1 shows an overhead view of the spiral coil and a cross-sectional view of the RF integrated inductor analyzed here. A (100)-oriented n-type silicon substrate (900～1000Ω·cm) with a 0.5μm thick wet thermal oxidized SiO_2 layer is used. 0.8μm thick Co_7ZrO_9 ferrite thin-film is spin-coated on the SiO_2 layer, which has a relative permeability of $\mu_r' = 4$, $\mu_r'' = 0.5$, a relative permittivity of $\varepsilon_r = 5$ at 1GHz, and an intrinsic FMR frequency above 2GHz. After RF-depositing a 150nm thick Cu/Ti seed layer, a 4μm thick Cu layer was electroplated on the ferrite thin-film to form the single-turn spiral coil, which has dimensions of 440μm × 440μm and a 20μm line width. Figure 2 shows an SEM photograph of the inductor sample. The reference air-core inductors are fabricated using similar processes without ferrite thin-film deposition.

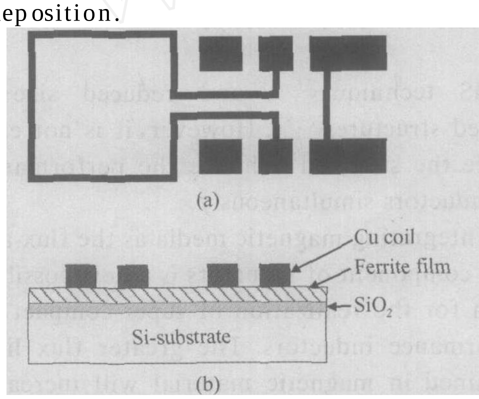

Fig. 1 Structure of RF integrated inductor with ferrite thin-film (a) Overhead view of the spiral coil; (b) Cross-sectional view

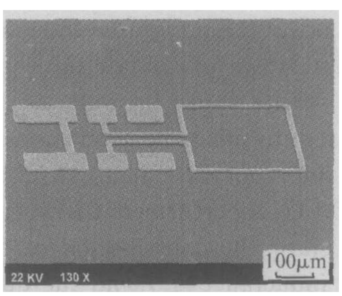

Fig. 2 SEM photograph of inductor sample with CoZrO thin-film

3 Equivalent circuit analysis

3.1 Air-core inductor

Figure 3 shows the basic equivalent circuit of an air-core on-chip spiral inductor[3]. L_s and R_s are the series inductance and resistance of the spiral. C_s is the series feedforward capacitance, taken as the combination of two parts: the overlap capacitance between the spiral and the center-tap underpass, and the interturn fringing capacitance. C_{ox} represents the capacitance of the oxide insulator layer between the spiral and the substrate. The silicon substrate capacitance and resistance are modeled as C_{Si} and R_{Si}.

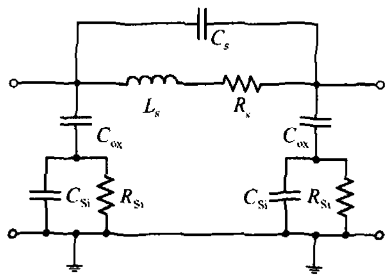

Fig. 3 Equivalent circuit of air-core on-chip spiral inductor

To demonstrate the inductor performance, concepts of quality factor (Q) and self-resonant frequency (f_0) are used. Q represents the net magnetic energy storing capability of the inductor. When Q vanishes to zero, the magnetic and electric energies are equal and the inductor is at self-resonance. This frequency is defined as f_0. From the equivalent circuit model, Q is derived as

$$Q = \text{metal factor} \times \text{substrate loss factor} \times \text{self-resonance factor} \tag{2}$$

where

$$\begin{cases} \text{metal factor} = \omega L_s / R_s \\ \text{substrate loss factor} = \dfrac{R_p}{R_p + \left[1 + (\omega L_s / R_s)^2\right] R_s} \\ \text{self-resonance factor} = \\ \qquad 1 - R_s^2 (C_s + C_p) / L_s - \omega^2 L_s (C_s + C_p) \end{cases} \tag{3}$$

In this expression, the metal factor accounts for the magnetic energy stored in the metal spiral and the ohmic loss due to its series resistance. The substrate loss factor represents the energy dissipated in the semiconductor silicon substrate. The self-resonance factor describes the reduction in Q as the frequency increases due to the increase of electric energy and the vanishing of Q at f_0. C_p and R_p are the equivalent series capacitance and series resistance of the shunt circuit including C_{ox}, C_{Si}, and R_{Si}:

$$\begin{cases} R_p = \dfrac{1}{\omega^2 C_{ox}^2 R_{Si}^2} + \dfrac{R_{Si}(C_{ox} + C_{Si})^2}{C_{ox}^2} \\ C_p = C_{ox} \dfrac{1 + \omega^2 (C_{ox} + C_{Si}) C_{Si} R_{Si}^2}{1 + \omega^2 (C_{ox} + C_{Si})^2 R_{Si}^2} \end{cases} \quad (4)$$

3.2 Ferrite thin-film inductor

Figure 4(a) shows the equivalent circuit of the on-chip spiral inductor with the under-spiral magnetic film, where the elements L_m, R_{loss}, C_m, R_m, R_{mc}, and C_{mlap} with the subscript "m" are added. L_m represents the inductance contribution of the magnetic material to the metal spiral, caused by the μ_r' of the magnetic thin-film. R_{loss} expresses the magnetic loss in the magnetic thin-film due to the μ_r''. They are in series with L_s and R_s. C_m and R_m symbolize the capacitance and resistance of the thin-film between the spiral and insulating layers. C_{mlap} represents the additional overlap capacitance introduced by the magnetic film. R_{mc} represents the ohmic loss due to the eddy current in the thin-film.

For ferrite thin-film, the resistivity is usually above $10^4 \Omega \cdot cm$, so the eddy current and the ohmic loss in the thin-film are small enough to be neglected. As a result, R_m and R_{mc} are left out as open branches. Then the circuit is simplified, as shown in Fig. 4(b), where L_{sm}, R_{sm}, C_{oxm}, C_{sm} are used to substitute the combined impedance of L_s and L_m, R_s and R_m, C_{ox} and C_m, C_s and C_{mlap}, respectively.

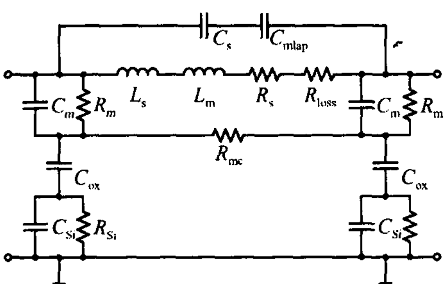

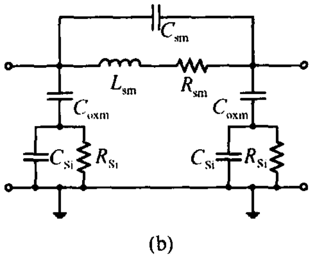

Fig. 4 Equivalent circuit of on-chip inductor with under-spiral magnetic thin-film (a) Modified two-port circuit with magnetic film added; (b) Simplified circuit of inductor with ferrite thin-film

Using current image and integral methods[9~12], the additional inductance L_m contributed from magnetic film to the inductor spiral can be derived as

$$L_m = \alpha L_s \quad (5)$$

The amplifying factor α is not only determined by the relative permeability μ_r and conductivity σ of the film, but also affected by the film's thickness and other structure parameters. For a semi-infinite nonconducting magnetic substrate, α is equal to $(\mu_r' - 1)/(\mu_r' + 1)$ [9], which means the upper limit of inductance enhancement of an inductor with under-spiral magnetic materials is nearly 100%, when μ_r' is high enough. For a magnetic thin-film with limited thickness, the enhancement is less. However, since the magnetic fluxes are mainly concentrated within a thin layer in proximity to the surface, a certain thickness of magnetic thin-film still ensures a significant enhancement of the inductance.

With the addition of the magnetic thin-film, the three terms in Q all change as

$$\begin{cases} \text{metal factor} = \omega L_{sm} / R_{sm} \\ \text{substrate loss factor} = \dfrac{R_{pm}}{R_{pm} + \left[1 + (\omega L_{sm}/R_{sm})^2\right] R_{sm}} \\ \text{self-resonance factor} = 1 - R_{sm}^2 (C_{sm} + C_{pm}) / L_{sm} \\ \qquad - \omega^2 L_{sm} (C_{sm} + C_{pm}) \end{cases} \quad (6)$$

where R_{pm} and C_{pm} are used to substitute for the combined impedance of C_{oxm}, C_{Si}, and R_{Si}. In the metal factor, both the numerator and denominator are increased. For typical ferrites, μ_r' is much greater than μ_r'' in the operating frequency region, which means the enhancement from L_s to L_{sm} governs the metal factor. Hence, the metal factor is increased significantly. The other two terms are affected by the ferrite thin-film's dielectric performance, represented by C_m in the equivalent circuit. In the substrate loss factor, R_{pm} increases a little due to the reduction from C_{ox} to C_{oxm}, if the silicon oxide is not changed and C_{ox} is fixed. As a result, the whole substrate loss factor increases slightly at operating frequencies far below f_0, where the R_{pm} governs the factor. As the frequency increases, the factor begins to decrease when the $\omega L_{sm}/R_{sm}$ begins to take effect, which causes a faster rate of descent than the air-core inductor without ferrite thin-film. The self-resonance factor has a similar change as the frequency increases. In addition, for ferrite thin-film in our experiments, the relative permittivity ε_r descends to a very low value which is near ε_r of SiO_2 at multi-GHz. This is helpful for the increase of the substrate loss factor and self-resonance factor at operating frequencies far below f_0. In conclusion, Q significantly improves due to the integration of ferrite thin-film. Meanwhile, the ferrite causes a slightly higher roll-off speed of Q and a slightly lower f_0 than in the inductor without ferrite thin-film.

4 Results and discussion

Two-port scattering parameters (*S*-parameters) of the inductors are tested by an Agilent E8358A network analyzer and Cascade Microtech coplanar ground-signal-ground probes with calibration performed up to the probe tips. The as-tested *S*-parameters are then changed to admittance parameters (*Y*-parameters). The pad de-embedding procedure is done by subtracting the *Y*-parameters of the open-pad pattern from those of the pad-embedded inductor[13]. Then the total inductance *L*, total resistance *R*, and *Q* are extracted according to the *Y* parameters

$$L = \frac{\mathrm{Im}(1/Y_{11})}{\omega} \tag{7}$$

$$R = \mathrm{Re}(1/Y_{11}) \tag{8}$$

$$Q = \frac{\mathrm{Im}(1/Y_{11})}{\mathrm{Re}(1/Y_{11})} \tag{9}$$

According to the equivalent circuit in Fig. 4(b), element parameters can also be extracted. For an inductor with a single layer, C_{sm} or C_s only contains the interturn capacitance, which is very small and is therefore neglected. Then the other parameters can be extracted as follows

$$L_{sm} = \omega^{1} \times \mathrm{Im}(-Y_{12}/|Y|) \tag{10}$$

$$R_{sm} = \mathrm{Re}(-Y_{12}/|Y|) \tag{11}$$

$$C_{pm} = \omega^{1} \times \mathrm{Im}(|Y|/Y_{11}) \tag{12}$$

$$R_{pm} = \mathrm{Re}(|Y|/Y_{11}) \tag{13}$$

Comparisons of L and Q between our sample with ferrite thin-film and the reference air-core inductor are shown in Fig. 5. The L of our sample is 2.02nH, which is 17% higher than that of the reference inductor, for which L = 1.72nH at 2GHz. L decreases slowly below 2GHz due to the skin effect in the metal spiral. Above 2GHz, L begins to increase to the resonant peak. Our sample yields a slightly steeper ascent because of its lower f_0, as demonstrated above. At 2GHz, the sample's Q is equal to 20.3, which is 40% higher than that of the reference inductor, for which Q = 14.5 at 2GHz. Above peak-Q frequency, Q decreases as the frequency increases due to the increased dissipation of electric energy. Our sample's Q decreases a little faster than that of the reference inductor, also due to the lower f_0. This agrees with the prediction from the equivalent circuit. Both f_0 of our sample and the reference inductor are greater than 9GHz. A detailed comparison of extracted parameters of our sample and the reference inductor at 2GHz is listed in Table 1.

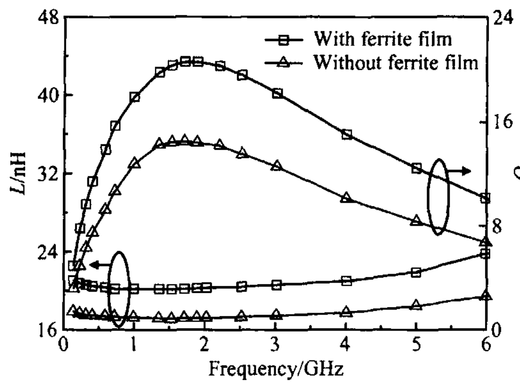

Fig. 5 Comparisons of L and Q between sample with ferrite film and reference inductor without ferrite film

Table 1 Comparison of measured parameters between sample and reference inductor at 2GHz

Parameter	Sample	Reference inductor
L / nH	2.02	1.72
R / Ω	1.3	1.5
Series inductance / nH	2.0 (L_{sm})	1.7 (L_s)
Series resistance / Ω	0.98 (R_{sm})	0.95 (R_m)
L_m / nH	0.3	—
R_m / Ω	0.03	—
C_{pm} or C_p / fF	76.1 (C_{pm})	79.3 (C_p)
R_{pm} or R_p / kΩ	3.8 (R_{pm})	1.1 (R_p)
Metal factor	25.6	22.5
Substrate loss factor	0.85	0.69
Self-resonance factor	0.96	0.97
Q	20.3	14.5

Experimental results indicate that the integration of ferrite thin-film in an RF integration inductor improves L and Q, which verifies the prediction of L and Q's amplifying effects from the equivalent circuit analysis. With the enhancement of L and Q, the size of on-chip inductors can be reduced efficiently.

5 Conclusion

We have derived an equivalent circuit for an RF integrated inductor with ferrite thin-film under the coil and presented a detailed analysis of the amplifying effects of the magnetic ferrite thin-film on L and Q of the inductor. Circuit element parameters were extracted from the RF measurements. Compared with the reference air-core inductor without magnetic film, L and Q of the ferrite thin-film inductor are 17% and 40% higher at 2GHz, respectively. Both the equivalent circuit analysis and test results demonstrate the significant enhancement of ferrite thin-film integration on the performance of an RF integration inductor. With the enhancement of L and Q, the size of on-chip inductors can be reduced efficiently.

References

[1] Liu F, Yang C, Ren T, et al. Fully integrated ferrite-based inductors for RF ICs. IEEE Conf Solid-State Sensors, Actuators and Microsystems, 2005: 895

[2] Liu Chang, Chen Xueliang, Yan Jinlong. Novel substrate pn junction isolation for RF integrated inductors on silicon. Chinese Journal of Semiconductors, 2001, 22: 1486 (in Chinese) [刘畅, 陈学良, 严金龙. 新颖的衬底 pn 结隔离型硅射频集成电感. 半导体学报, 2001, 22: 1486]

[3] Yue C P, Wong S S. On-chip spiral inductors with patterned ground shields for Si-based RF IC's. IEEE J Solid-State Circuits, 1998, 33: 743

[4] Huo X, Chen K J, Chan P C. High-Q copper inductors on standard silicon substrate with a low-k BCB dielectric layer. IEEE MTT-S, 2002: 513

[5] Yoon J B, Choi Y S, Kim B I, et al. CMOS-compatible surface-micromachined suspended-spiral inductors for multi-GHz silicon RF ICs. IEEE Electron Device Lett, 2002, 23: 591

[6] Jiang H, Wang Y, Yeh J A, et al. On-chip spiral inductors suspended over deep copper-lined cavities. IEEE Trans Microw Theory Tech, 2000, 48: 2415

[7] Burghartz J N, Jenkins K A, Soyuer M. Multilevel-spiral inductors using VLSI interconnect technology. IEEE Electron Device Lett, 1996, 17: 428

[8] Zolfaghari A, Chan A, Razavi B. Stacked inductors and transformers in CMOS technology. IEEE J Solid-State Circuits, 2001, 36: 620

[9] Roshen W A, Turcotte D E. Planar inductors on magnetic substrates. IEEE Trans Magn, 1988, 24: 3213

[10] Roshen W A. Effect of finite thickness of magnetic substrate on planar inductors. IEEE Trans Magn, 1990, 26: 270

[11] Hurley W G, Duffy M C. Calculation of self and mutual impedances in planar magnetic inductors. IEEE Trans Magn, 1995, 31: 2416

[12] Hurley W G, Duffy M C. Calculation of self- and mutual impedances in planar sandwich inductors. IEEE Trans Magn, 1997, 33: 2282

[13] Wijnen P J, Claessen H R, Wolsheimer E A. A new straightforward calibration and correction procedure for "on wafer" high frequency S-parameter measurements (45MHz-18GHz). IEEE Bipolar Circuits and Technology Meet, 1987: 70

铁氧体磁膜 RF 集成微电感等效电路分析 *

任天令[1,†]　杨　晨[1]　刘　锋[1]　刘理天[1]　王自惠[2]　张　筱[3]

(1 清华大学微电子学研究所, 北京　100084)

(2 伊利诺理工学院电气与计算机工程系, 芝加哥 IL　60616, 美国)

(3 清华大学电子工程系, 北京　100084)

摘要: 针对已制作并发表的一种新型铁氧体磁膜结构射频集成微电感进行了等效电路分析. 阐述了磁性铁氧体薄膜对电感的感值(L)和品质因数(Q)的增强作用. 对射频测试结果进行了电路元件参数提取. 结果表明, 与空气芯无磁膜微电感相比, 磁膜结构微电感的 L 和 Q 在 2GHz 处分别提高了 17%和 40%. 等效电路分析和测试结果均证明了铁氧体薄膜的引入对增强射频集成微电感性能的作用显著.

关键词: 电感; 等效电路; 铁氧体薄膜; 射频集成电路

EEACC: 2560B; 2140; 3110E

中图分类号: TN409　**文献标识码**: A　**文章编号**: 0253-4177(2006)03-0511-05

* 美国自然科学基金资助项目(批准号:0302449)

† 通信作者. Email: RenTL@tsinghua.edu.cn

2005-11-07 收到